

# Comparative study of electropolymerized cobalt porphyrin and phthalocyanine based films for the electrochemical activation of thiols

Sophie Griveau,<sup>a</sup> Valérie Albin,<sup>a</sup> Thierry Pauporté,<sup>a</sup> José H. Zagal<sup>b</sup> and Fethi Bedioui<sup>\*a</sup>

<sup>a</sup>Laboratoire d'Electrochimie et Chimie Analytique, UMR CNRS-ENSCP n° 7575, Ecole Nationale Supérieure de Chimie de Paris, 11 Rue Pierre et Marie Curie, 75231 Paris, Cedex 05, France. E-mail: bedioui@ext.jussieu.fr

<sup>b</sup>Departamento de Química de los Materiales, Facultad de Química y Biología, Universidad de Santiago de Chile, Casilla 40, Correo 33 Santiago, Chile

Received 27th July 2001, Accepted 6th November 2001  
First published as an Advance Article on the web 7th January 2002

We present a comparative study of the behavior of electrodes modified with electropolymerized cobalt porphyrins and cobalt phthalocyanine films towards the electro-oxidation of 2-mercaptoethanol (2-ME). First, we report here on the electrochemical formation of the complex-based films and their characterization by cyclic voltammetry and electrochemical quartz microbalance measurements. The obtained results clearly show that the accessibility to the redox centers within the electropolymerized films is limited to the external layers. In particular, this report focuses on the effect of polymer film thickness on the thiol electro-oxidation reaction. However, the electrocatalytic activity of the porphyrin-modified electrode depends on the film thickness, in contrast to the phthalocyanine-based ones: the greater the thickness the lower is the activation of the thiol in terms of current and of oxidation potential. This can be explained by the lower electronic conductivity of electropolymerized porphyrin films compared to the phthalocyanine-based ones, and the probable intervention of the Co<sup>III</sup> form of the deposited complexes.

## Introduction

Metalloporphyrins are widely studied as biomimetic models for several biological redox processes, such as the activation of molecular oxygen.<sup>1</sup> They have been developed as efficient catalysts for the oxidative degradation of various types of pollutants and residual wastes.<sup>2</sup> Related complexes such as metallophthalocyanines were also reported to be efficient catalysts,<sup>3</sup> especially for the electrochemical oxidation of thiols.<sup>4–8</sup> Indeed, the electrochemical detection and/or activation of thiol-derived substances is an important field of research as they can be present as contaminants in fuels and biological fluids and they may be useful as markers of food deterioration. For this purpose, it has been reported that modified electrodes coated by adsorbed cobalt phthalocyanines show substantial electrocatalytic activity for the electro-oxidation of thiols such as L-cysteine, 2-mercaptoethanol and reduced glutathione,<sup>4</sup> by lowering particularly the overpotential of the electrochemical processes. Only few attempts have been reported to attempt to develop the use of multilayered-based metallophthalocyanine films for the activation of thiols, to offer a better alternative to the design of efficient and stable electrocatalysts.<sup>9–14</sup> In this context, in a recent work we explored the electrocatalytic activity of electropolymerized cobalt tetraaminophthalocyanine (CoTAPc, see structure in Fig. 1) films for the oxidation of 2-mercaptoethanol (2-ME)<sup>14</sup> and reported a comparative study of these chemically modified electrodes as a function of CoTAPc film thickness. Our results showed that only external layers located on the film/solution interface are electrocatalytically active towards the thiol oxidation. Indeed, there was no substantial increase in the faradaic currents by increasing the film thickness. Thus, there is no participation of the CoTAPc located in the bulk of the film. Our study constitutes one of the very rare examples of such an investigation.<sup>14</sup>

In a very recent study, we have extended the use of

electropolymerized cobalt porphyrin film-coated electrodes for the electrocatalysis of the oxidation of 2-ME<sup>15</sup> and our preliminary results showed, for the first time, that the cobalt porphyrin modified electrode possesses potential electrocatalytic activity. Although the activity of the films is lower than that of the phthalocyanine-based ones, these results demonstrated the potential application of the examined electrodes for the electrochemical activation of thiols.

We explore in this study the electrocatalytic activity of electropolymerized CoTHPP and CoTAPP films (CoTHPP = cobalt tetrakis(*p*-hydroxyphenyl)porphyrin; CoTAPP = cobalt tetrakis(*o*-aminophenyl)porphyrin, see structures in Fig. 1) for the oxidation of 2-ME. We report here a comparative study of the electrocatalytic behavior of these modified electrodes with that of electropolymerized CoTAPc films, with emphasis on the effects of the film thickness on the electro-oxidation process. UV-visible spectroscopy, electrochemical quartz microbalance (EQCM) and cyclic and rotating disk electrode voltammeteries enabled the full characterization of the examined films.

## Experimental

CoTHPP, CoTAPP and CoTAPc were purchased from Mid-century Chemical Co. (Posen, IL, USA) and used without further purification. All other products were reagent grade and used as received. The working electrode was a vitreous carbon disk electrode from Radiometer-Tacussel (France) exposing a geometrical area of 0.071 cm<sup>2</sup> and mounted in Teflon<sup>®</sup>. The electrode was polished before each experiment with 3 and 0.3 μm alumina pastes followed by extensive rinsing with ultra-pure Milli-Q water. The electrochemical experiments were carried out with a conventional three-electrode cell and a Princeton Applied Research Inc. potentiostat/galvanostat model 263A (USA). Platinum wire was used as counter

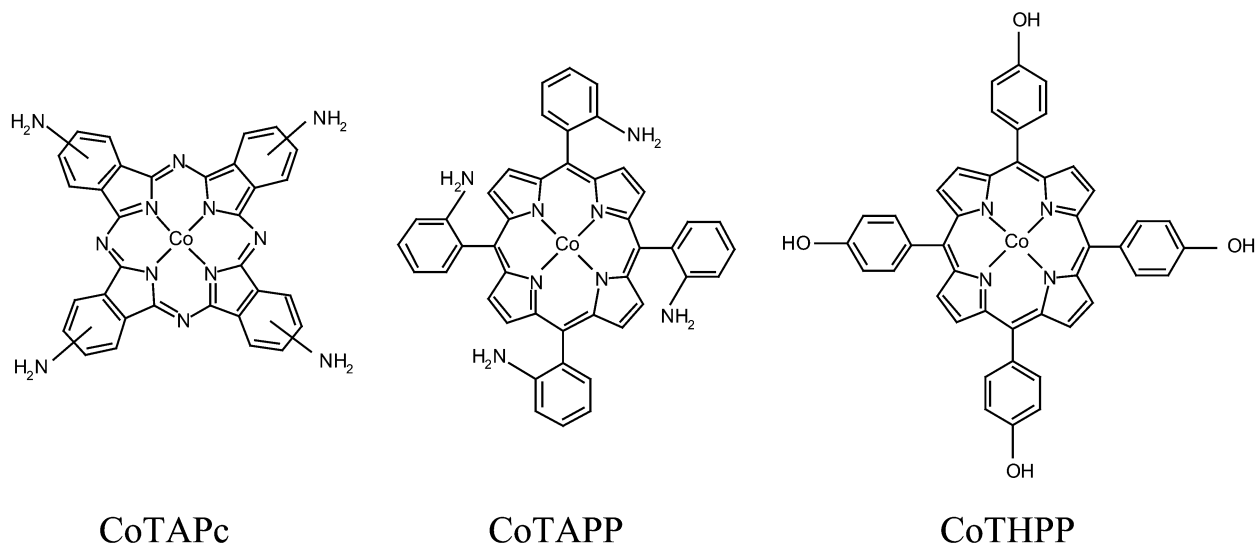


**Fig. 1** Structures of CoTAPc (cobalt tetraaminophthalocyanine), CoTAPP (cobalt tetrakis(*o*-aminophenyl)porphyrin) and CoTHPP (cobalt tetrakis(*p*-hydroxyphenyl)porphyrin).

electrode and saturated calomel electrode (SCE) as reference electrode. Electrolytic solutions were routinely deoxygenated with argon. All the potential values are given *versus* the saturated calomel electrode (SCE).

CoTAPc, CoTAPP and CoTHPP were adsorbed on vitreous carbon by placing a drop of a 1 mmol L<sup>-1</sup> of the complex in dimethylformamide (for CoTAPc) or acetonitrile (for the cobalt porphyrins) for 1 min on the surface. After this, the excess of complex was removed with DMF or acetonitrile, followed by rinsing with ethanol. We should note here that, as we have previously reported,<sup>16</sup> there may be a drastic influence of the vitreous carbon electrode polishing on the amount of the electrochemically active adsorbed complexes and their electrocatalytic behavior. Also, both the vitreous carbon electrode polishing and the starting monomer solution have a great influence on the initiation of the electropolymerization process. We have scrupulously paid attention to these facts in order to have accurate and reproducible measurements, and make this study self consistent.

Experiments were also conducted on ITO conductive glass electrodes (Solems, France) to obtain the UV-visible transmission spectra of the electropolymerized films of various thickness. *In situ* spectroelectrochemical measurements were carried out in a home made cell consisting of a standard UV-Visible cuvette (path length of 1 cm and total solution volume of 5.5 mL) with an opening on the top to facilitate the introduction of the working, reference and counter electrodes. The working electrode was a ITO conductive glass of geometrical area 0.8 cm (width) × 5 cm (length), which was flattened against one of the walls of the cuvette orthogonal to the light beam pathway. A platinum wire was used as the counter electrode and a home-made AgCl coated Ag wire as reference electrode. The potential difference between this reference electrode and SCE was equal to +145 mV and checked daily, before and after use. Electrolytic solutions were routinely deoxygenated with argon and kept under inert atmosphere during the experiments. UV-Visible data were recorded by using a Shimadzu UV-160A spectrophotometer.

For the EQCM experiments, we used the same experimental set up developed previously.<sup>17</sup> In brief, a standard three-electrode cell with a gold working electrode of surface area 1.37 cm<sup>2</sup> was used (Maxlek Inc., USA). The gold surface quartz microbalance was covered with an ultrathin layer (30 nm) of carbon deposited by evaporation in order to model the carbon surfaces of the microelectrodes. A platinum wire served as the counter electrode. The reference electrode was a saturated calomel electrode. Sweep voltammetry investigations were

performed using an EG & G Princeton Applied Research model 372A system. The quartz crystal was AT cut with an operating frequency of 5 MHz. The resonance frequency was measured with a Maxtek model PM710 connected to a personal computer. The frequency changes,  $\Delta f$ , are proportional to the mass changes,  $\Delta m$ , according to the Sauerbrey equation,<sup>18</sup> and the ratio  $\Delta m/\Delta f$  has been evaluated to 18 ng cm<sup>-2</sup> Hz<sup>-1</sup> after a thorough calibration of the oscillating quartz crystals.<sup>19-21</sup> The viscoelastic properties of the films in the frequency response has been neglected in this work owing to the small thickness of the examined layers.

## Results and discussion

### Electropolymerization and characterization of the films

Fig. 2 shows consecutive cyclic voltammograms obtained at a vitreous carbon electrode in: (i) dimethylformamide (DMF) + 0.1 mol L<sup>-1</sup> tetrabutylammonium tetrafluoroborate (TBABF<sub>4</sub>) solution containing 1 mmol L<sup>-1</sup> CoTAPc (Fig. 2a); (ii) acetonitrile (ACN) + 0.1 mol L<sup>-1</sup> TBABF<sub>4</sub> solution containing 1 mmol L<sup>-1</sup> CoTAPP (Fig. 2b) and (iii) ACN + 0.1 mol L<sup>-1</sup> TBABF<sub>4</sub> solution containing 1 mmol L<sup>-1</sup> CoTHPP (Fig. 2c). The build up of the electropolymerized poly-CoTAPc, poly-CoTAPP and poly-CoTHPP can be followed by the increase in the voltammetric currents. Electropolymerization of CoTAPc was achieved by repetitive cycling of the potential of the vitreous carbon electrode between -0.2 and +0.9 V at 0.2 V s<sup>-1</sup> and repeated cycling around the CoTAPc ligand oxidation (around 0.6–0.9 V) results in the polymerization of the complex *via* its oxidized amino groups and the deposition of an electroactive polymer on the electrode surface.<sup>14</sup> Electropolymerization of CoTHPP and CoTAPP was achieved by repeated potential scans between 0 and +1.3 V and 0 and +1.1 V, respectively (at 0.2 V s<sup>-1</sup>). The repeated cycling around the anodic limit of the potential range results in the oxidation of the hydroxyphenyl or the aminophenyl groups, respectively, leading to the deposition of the corresponding electroactive polymers on the electrode surface.<sup>22-26</sup> Thus, different polymer thickness can be obtained by controlling the number of the electropolymerizing scans.

Simultaneous piezoelectric microgravimetry and cyclic voltammetry measurements at an electrochemical quartz crystal microbalance have been used to monitor the growth of poly-CoTAPc, poly-CoTHPP and poly-CoTAPP films, during potential cycling. Thus, formation of the electropolymerized films can be followed by microgravimetry as illustrated in

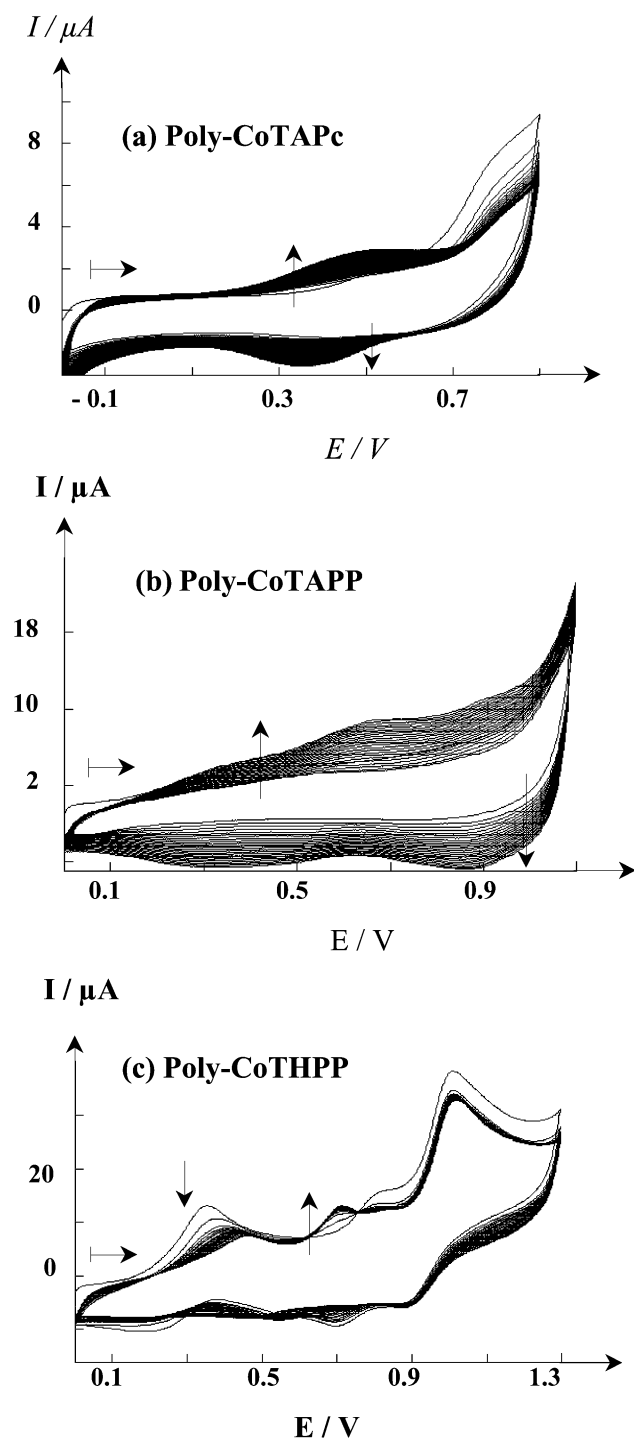


Fig. 2 Cyclic voltammetry at vitreous carbon disk electrode of (a)  $1 \text{ mmol L}^{-1}$  CoTAPc in DMF +  $0.1 \text{ mol L}^{-1}$  TBABF<sub>4</sub>, (b)  $1 \text{ mmol L}^{-1}$  CoTAPP in ACN +  $0.1 \text{ mol L}^{-1}$  TBABF<sub>4</sub> and (c)  $1 \text{ mmol L}^{-1}$  CoTHPP in ACN +  $0.1 \text{ mol L}^{-1}$  TBABF<sub>4</sub>. Scan rate  $0.2 \text{ V s}^{-1}$ .

Fig. 3. The mass uptake results, from the resonant frequency shift according to the Sauerbrey equation give surface coverages of  $8.34$ ,  $620$  and  $50 \text{ ng cm}^{-2} \text{ scan}^{-1}$  of CoTAPc, CoTAPP and CoTHPP, respectively. By taking into account the size and the shape of the square planar complexes ( $20 \times 20 \text{ \AA}^2$  for the porphyrins) and the average distance between two stacked moieties ( $4 \text{ \AA}$ ),<sup>27–29</sup> one can estimate the thickness of the deposit to vary by  $8.4$  and  $0.6 \text{ nm scan}^{-1}$ , or the equivalent of  $21$  and  $1.5$  monolayers of complex  $\text{scan}^{-1}$  for poly-CoTAPP and poly-CoTHPP, respectively. It should be noted that the very low coverage of the carbon-coated golden quartz microbalance crystal by CoTAPc is due to the very poor adherence of the electropolymerized complex, so that the

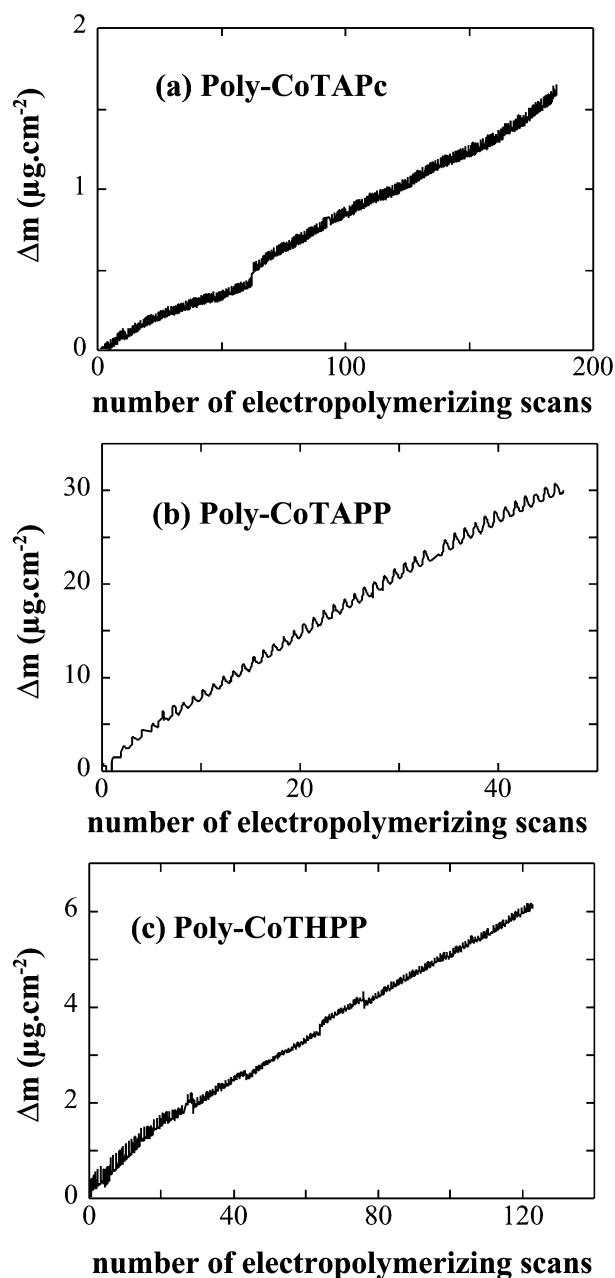


Fig. 3 Evolution of deposited mass of CoTAPc (curve a), CoTAPP (curve b) and CoTHPP (curve c) versus the number of electropolymerizing scans (same electropolymerization conditions as Fig. 2).

thickness of the deposit per scan does not lead to a significant value. We have previously reported that typical thicknesses of poly-CoTAPc deposits growth on ITO, measured by scanning electron microscopy on dry films are *ca.*  $2.5 \text{ nm scan}^{-1}$ ,<sup>14</sup> or the equivalent  $6.25$  monolayers  $\text{scan}^{-1}$ . The formation of the complex-based films on ITO transparent electrodes was confirmed by UV-visible spectrophotometry. This is exemplified in the case of poly-CoTAPP, as shown in Fig. 4. The absorption spectrum of CoTAPP in ACN solution is compared with that of the poly-CoTAPP films, prepared by  $24$ ,  $48$ ,  $80$  and  $160$  electropolymerizing scans on a transparent ITO electrode. The intensity of the absorption bands do increase linearly over the first  $100$  electropolymerizing scans (and then increase further but not linearly), indicating that the electropolymerization process progresses during the cycling of the potential (data not shown). The similarity between the spectra of the monomer and that of the polymer indicates that the structure of the complex, upon electropolymerization remains almost the same. In the case of the Soret band, a peak broadening is observed

## Absorbance

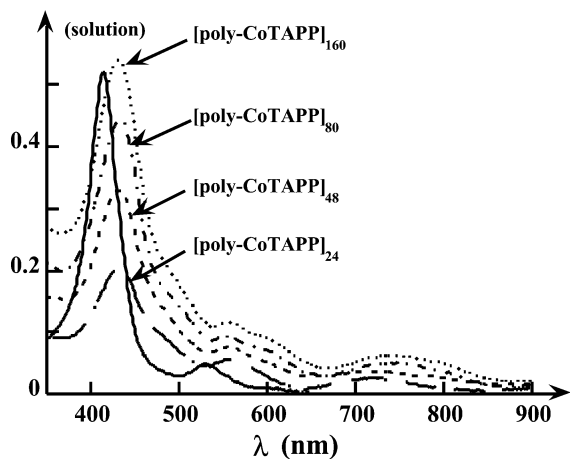


Fig. 4 Absorption spectra of poly-CoTAPP films on ITO electrodes immersed in ACN. The straight line curve corresponds to CoTAPP monomer in ACN solution.

with an hyperchromic shift. Considerable broadness of the Soret band was previously observed for several supported porphyrins<sup>28–31</sup> and was attributed to some degree of aggregation and stacking of the porphyrin molecules on the electrode surface. The similarity of the polymer and monomer spectra indicates that the structure of the complex unit has remained intact upon electropolymerization.

Fig. 5 shows the cyclic voltammograms of various electropolymerized [poly-CoTAPC]<sub>n</sub>, [poly-CoTAPP]<sub>n</sub> and [poly-CoTHPP]<sub>n</sub> films in 0.5 mol L<sup>-1</sup> NaOH aqueous solution (the subindex *n* indicates the number of electropolymerizing scans) recorded by starting the potential scanning from -1.30 to +0.1 V. For each complex the modified electrodes exhibit cyclic voltammograms which have similar shape. As previously reported in the case of poly-CoTAPc, the cyclic voltammograms exhibit two pairs of peaks at *ca.* -0.72 and *ca.* -0.26 V (Fig. 5a), respectively. The well-defined pair of peaks located at *ca.* -0.72 V is related to the Co<sup>II</sup>/Co<sup>I</sup> redox process<sup>14</sup> whereas there is no agreement in the literature about the nature of the redox process located at *ca.* -0.26 V.<sup>32</sup> For poly-CoTHPP and poly-CoTAPP, the cyclic voltammograms exhibit two couples of peaks at *ca.* -1.05 and *ca.* -0.20 V (Fig. 5b and c), respectively. By comparison to similar polypyrrole-based cobalt porphyrin films,<sup>22,28,29,33</sup> the pair of peaks located at *ca.* -1.05 V can be attributed to the Co<sup>III</sup>/Co<sup>I</sup> redox process, whereas the second pair at *ca.* -0.20 V is related to the Co<sup>III</sup>/Co<sup>II</sup> redox process. This process presents a lower reversibility, compared to the Co<sup>II</sup>/Co<sup>I</sup> transition (the difference between the potential values of the oxidation and reduction peaks  $\Delta E_p$  equals 140 mV at 100 mV s<sup>-1</sup>, for [poly-CoTHPP]<sub>24</sub> for example). Also, the peak intensities are smaller than that corresponding to the Co<sup>II</sup>/Co<sup>I</sup> couple. As far as we are aware, there are very few studies that have discussed the poor reversibility of the Co<sup>III</sup>/Co<sup>II</sup> redox couple, compared to that of the Co<sup>II</sup>/Co<sup>I</sup> couple.<sup>33</sup> For example, such a behavior has been reported for cobalt tris-bipyridine complexes immersed in polymer films<sup>34</sup> and also for polymeric cobalt tetraphehypporphyrins.<sup>22,28</sup> Thus, the rather slow behavior of the Co<sup>III</sup>/Co<sup>II</sup> electrochemical process is not unusual.

The amount of electroactive redox cobalt complex sites can be estimated from the electrical charge under the oxidative (or reductive) Co<sup>II</sup>/Co<sup>I</sup> peak shown in Fig. 5 (see inserts). For the examined films, the peak current intensities relative to the Co<sup>II</sup>/Co<sup>I</sup> redox process are proportional to the potential scan rate *v*, for *v* varying from 10 to 500 mV s<sup>-1</sup>, and the electrical charges *Q* (under the oxidative or reductive Co<sup>II</sup>/Co<sup>I</sup> peak) independent of *v*, for *v* varying from 10 to 100 mV s<sup>-1</sup> and slightly decrease for higher rates. This is indicative of an immobilized

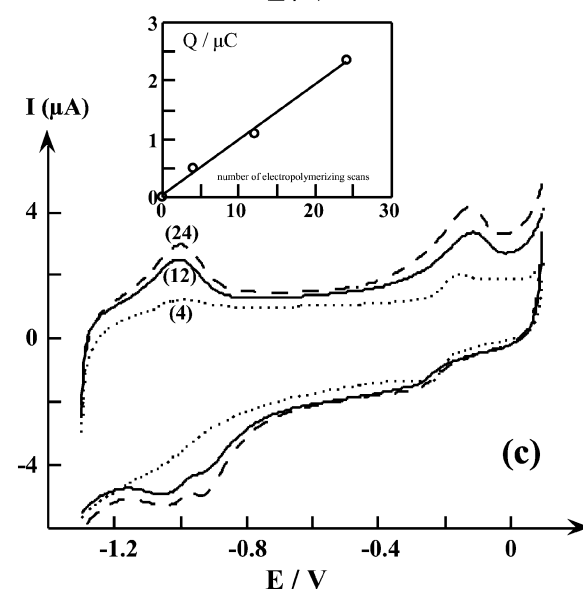
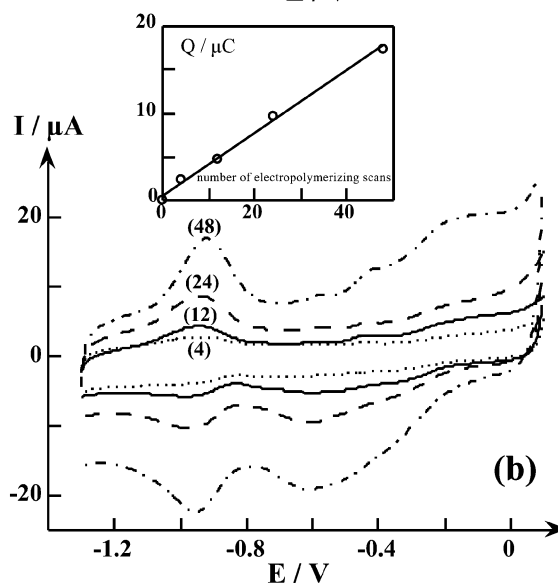
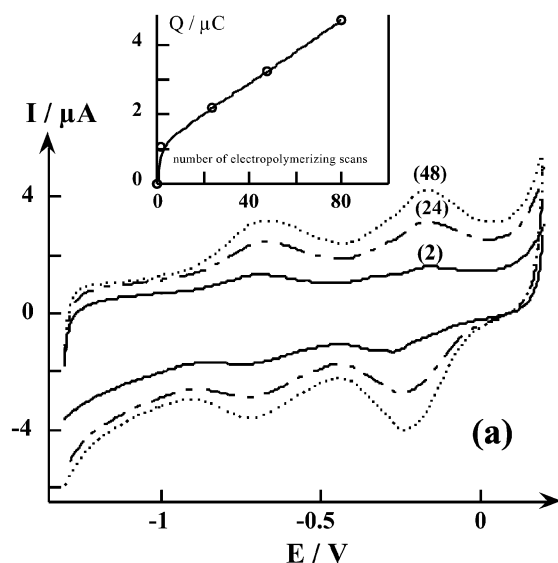


Fig. 5 Cyclic voltammograms of (a) poly-CoTAPc-vitreous carbon modified electrodes, (b) poly-CoTAPP-vitreous carbon modified electrodes and (c) poly-CoTHPP-vitreous carbon modified electrodes in 0.5 mol L<sup>-1</sup> NaOH (scan rate 0.1 V s<sup>-1</sup>). Numbers in parentheses indicate the number of electropolymerizing scans.

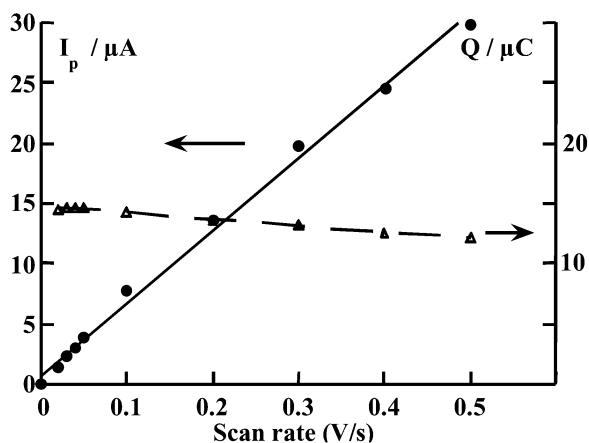


Fig. 6 Evolution of peak current intensity  $I_p$  (●) and electrical charge  $Q$  (Δ) with potential scan rate for the anodic peak of the  $\text{Co}^{\text{I}}/\text{Co}^{\text{II}}$  redox process of a [poly-CoTAPP]<sub>24</sub> film.

monolayer-like behavior,<sup>35,36</sup> as exemplified in Fig. 6 for the [poly-CoTAPP]<sub>24</sub> film. Thus, calculations of the total amounts of apparent electroactive sites give valid indications of values ranging from  $7.46 \times 10^{-11}$  to  $255.35 \times 10^{-11} \text{ mol cm}^{-2}$ , depending on the complex and the number of electropolymerizing scans (see Table 1 where full details of the electrochemical characterization of the different modified electrodes are given). The amount of electroactive CoTAPP and CoTHPP represent only 6 and 22% of the total deposited amount (estimated by EQCM experiments). This indicates that as the films grow, a considerable fraction of the complexes remains electrochemically inactive, if one assumes that the rate of the electropolymerization process is not affected by the nature of the electrode materials. It is likely that only few monolayers, probably those located at the external film surface/solution interface, are electrochemically active. This is probably due to the fact that the redox processes require the exchange of counter ions and this becomes more difficult for complex units which are buried inside the polymer. Again, by taking into account the size and the shape of the cobalt complexes, one may estimate the thickness of the electroactive part of the deposits to vary from 0.72 to 24.60 nm, or the equivalent of 1.8 to 61.5 monolayers of complex (see Table 1).

Further analysis of the electropolymerized films was provided by cyclic and rotating disk electrode voltammeteries of anionic and cationic electroactive probes in solution, namely  $\text{Fe}(\text{CN})_6^{4-}$  and  $\text{Ru}(\text{NH}_3)_6^{3+}$ . This was aimed at attempting to

**Table 1** Electrochemical characteristics of electropolymerized poly-CoTAPc, poly-CoTAPP and poly-CoTHPP film modified vitreous carbon electrodes in  $0.5 \text{ mol L}^{-1}$  NaOH aqueous solution (the subindex indicates the number of electropolymerizing scans used for the electrode modification)

Modified electrode	Apparent electroactive amount of complex/ $10^{11} \text{ mol cm}^{-2}$ <sup>a</sup>	Film thickness/ nm <sup>b</sup>	Film thickness/ nm <sup>c,d</sup>
[poly-CoTAPc] <sub>2</sub>	15.21	0.5	5 <sup>d</sup>
[poly-CoTAPc] <sub>24</sub>	31.97	1.1	60 <sup>d</sup>
[poly-CoTAPc] <sub>48</sub>	47.32	1.6	120 <sup>d</sup>
[poly-CoTAPP] <sub>4</sub>	34.50	3.3	33.6 <sup>c</sup>
[poly-CoTAPP] <sub>12</sub>	70.42	6.8	100.8 <sup>c</sup>
[poly-CoTAPP] <sub>24</sub>	141.59	13.6	201.6 <sup>c</sup>
[poly-CoTAPP] <sub>48</sub>	255.35	24.6	403.2 <sup>c</sup>
[poly-CoTHPP] <sub>4</sub>	7.46	0.7	2.4 <sup>c</sup>
[poly-CoTHPP] <sub>12</sub>	16.05	1.5	7.2 <sup>c</sup>
[poly-CoTHPP] <sub>24</sub>	34.22	3.3	14.4 <sup>c</sup>

<sup>a</sup>Calculated from cyclic voltammetry experiments at  $0.1 \text{ V s}^{-1}$ . <sup>b</sup>Measured from cyclic voltammetry experiments. <sup>c</sup>Measured from EQCM experiments. <sup>d</sup>Estimated from measurements done by scanning electron microscopy (ref 14).

give further insights on the possible electron transfer mediation by the redox polymer modified electrode either at the solution-film interface or throughout the bulk of the film. The cyclic voltammograms of ferrocyanide,  $\text{Fe}(\text{CN})_6^{4-}$  in solution obtained on uncoated vitreous carbon electrode and on modified electrodes (poly-CoTAPc, poly-CoTAPP and poly-CoTHPP prepared by different electropolymerizing scans) showed some variations in their shape. This is exemplified in Fig. 7 for poly-CoTAPP films. It appears that the direct oxidation of ferrocyanide is accomplished on [poly-CoTAPP]<sub>12</sub> modified electrode (curve c) with an obvious loss of reversibility, compared to the very thin [poly-CoTAPP]<sub>4</sub> film (curve b) or the bare vitreous carbon electrode (similar to curve b; data not shown). Thus, the characteristics of the ferri/ferrocyanide redox process in solution depends on the modification of the vitreous carbon electrode surface, and more precisely on the polymer film thickness. Similar results were obtained on poly-CoTHPP films, either with  $\text{Fe}(\text{CN})_6^{4-}$  or  $\text{Ru}(\text{NH}_3)_6^{3+}$  as electroactive probes in solution (data not shown). Hydrodynamic voltammetric studies of ferri/ferrocyanide on rotating poly-CoTAPc,<sup>14</sup> poly-CoTAPP and poly-CoTHPP modified electrodes showed, by using Koutecky–Levich plots of  $1/I_L$  ( $I_L$  is the limiting current) versus  $1/(\text{rotation rate})^{1/2}$ ,<sup>37</sup> that the electrochemical oxidation of  $\text{Fe}(\text{CN})_6^{4-}$  is accomplished under solution mass-transport control, without complications due to diffusion limitations inside the polymer films. Also, the Koutecky–Levich plots for kinetics currents measured at various different potential values at the foot of the hydrodynamic waves are straight lines with non-zero ordinates. This suggests again the changes in the electron transfer rate reaction at the modified electrodes.<sup>38</sup> These observations indicate a slowing in the electron transfer kinetics of the examined probes on the modified electrodes induced by the low conductive hydroxyphenyl- and aminophenyl-substituted porphyrin based films. They also may be indicative of the fact that the films are rather compact, or that the pores are smaller than the electroactive probe ions. Indeed, the blocking characteristics of the thin complex-based films may arise from the film structure itself consisting of a homogeneous membrane or pinholes holding matrix.<sup>35</sup> Further experiments are needed to distinguish between these various situations.

At this point of the study, the remarkable result is that the EQCM, UV-visible and cyclic voltammetry data demonstrate that a limited amount of cobalt complexes is electroactive, in the various electropolymerized films. This confirms previously

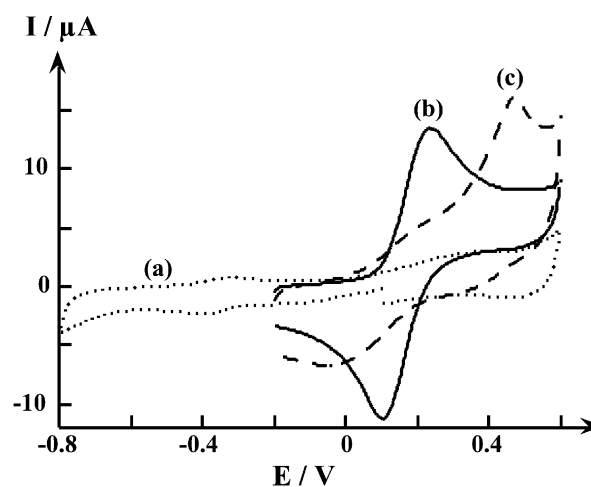
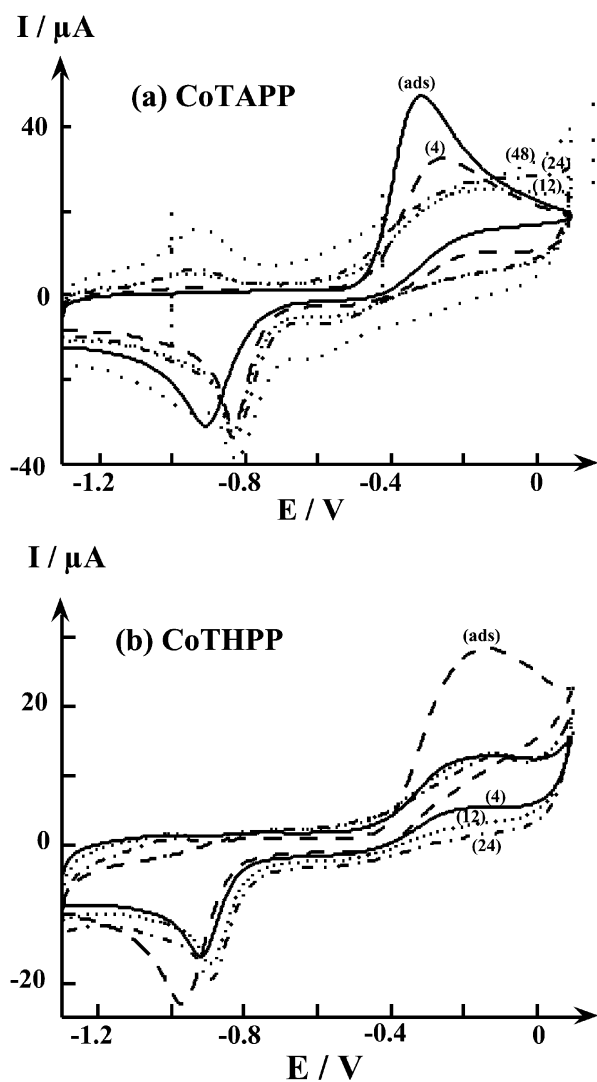


Fig. 7 Cyclic voltammograms of (a) [poly-CoTHPP]<sub>12</sub>-vitreous carbon modified electrode in phosphate buffer ( $0.1 \text{ mol L}^{-1}$ ;  $\text{pH} = 7.4$ ), (b) [poly-CoTHPP]<sub>4</sub>-vitreous carbon modified electrode in phosphate buffer ( $0.1 \text{ mol L}^{-1}$ ;  $\text{pH} = 7.4$ ) containing  $\text{Fe}(\text{CN})_6^{4-}$  ( $1 \text{ mmol L}^{-1}$ ), (c) [poly-CoTHPP]<sub>12</sub>-vitreous carbon modified electrode in phosphate buffer ( $0.1 \text{ mol L}^{-1}$ ;  $\text{pH} = 7.4$ ) containing  $\text{Fe}(\text{CN})_6^{4-}$  ( $1 \text{ mmol L}^{-1}$ ). Scan rate  $0.1 \text{ V s}^{-1}$ .

reported results reported indicating that as the films grow, a considerable fraction of it remains electrochemically inactive. All this suggests that the cobalt complex-based films are very dense and then only very few monolayers, probably those located at the external film surface/solution interface, are electrochemically active (*i.e.* accessible). For the porphyrin-based films, poly-CoTHPP and poly-CoTAPP, only a low conductivity is observed.

#### Electrocatalytic oxidation of 2-mercaptoethanol on the electropolymerized films

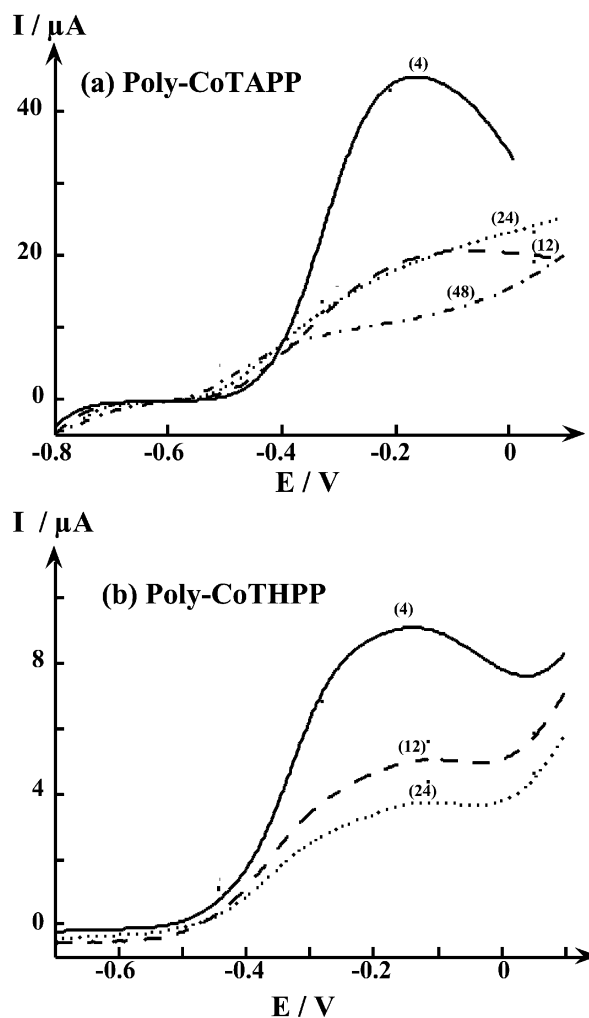
Fig. 8 illustrates the effect of adding 2-ME ( $1 \text{ mmol L}^{-1}$ ) to the  $0.5 \text{ mol L}^{-1}$  NaOH aqueous solution, on poly-CoTAPP and poly-CoTHPP modified electrode activity. Under these conditions, a large oxidation current is observed as soon as  $-0.45 \text{ V}$ , which is related to the electrocatalytic oxidation of 2-ME at the cobalt porphyrin-based electrodes.<sup>15</sup> These data illustrate also the effect of film thickness on the electrocatalytic properties of poly-CoTAPP and poly-CoTHPP. The responses of the adsorbed layers of the complexes, which have not been electropolymerized, are also shown. It should be noted that no electro-oxidation current related to the oxidation of 2-ME on vitreous carbon bare electrode is observed in the investigated potential range, as has been previously reported.<sup>14,15</sup> The first point that should be emphasized here is that the most active electrode (in terms of current and of peak potential) is



**Fig. 8** Effect of the thickness of electropolymerized poly-CoTAPP (a) and poly-CoTHPP (b) films on the electro-oxidation of 2-mercaptoethanol ( $1 \text{ mmol L}^{-1}$  in  $0.5 \text{ mol L}^{-1}$  NaOH; scan rate  $0.1 \text{ V s}^{-1}$ ).

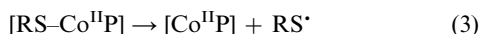
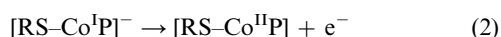
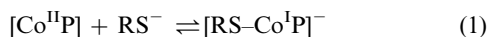
that modified with an adsorbed layer of the cobalt porphyrins. The second important point is that the activities of the electropolymerized films do not improve with their thickness; by contrast, a slight decrease is observed. Thus, as suggested above, not all the cobalt centers imbedded inside the films of poly-CoTAPP and poly-CoTHPP are electrochemically active. Only few external layers located on the film/solution interface are electrocatalytically active towards 2-ME oxidation. Indeed, there is no substantial increase in the faradaic currents by increasing the film thickness. Thus, there is no participation of the cobalt complexes located in the bulk of the dense, non porous films. In addition, it can also be noticed that, as was previously reported for cobalt phthalocyanine,<sup>14</sup> the porphyrin-based films are not only active for the electro-oxidation of 2-mercaptoethanol but they are also active for the electro-reduction of the corresponding disulfide, as revealed by the cathodic peak at *ca.*  $-0.9 \text{ V}$ . The assignment of this reduction peak to disulfide was clearly verified by studying the electroreduction of 2-hydroxyethyl disulfide (with no 2-ME in solution) at various cobalt phthalocyanine modified electrodes.<sup>39</sup>

Fig. 9 shows the evolution of the hydrodynamic voltammograms obtained on rotating disk poly-CoTAPP and poly-CoTHPP modified electrodes in presence of 2-ME in  $0.5 \text{ mol L}^{-1}$  NaOH aqueous solution. The shape of the voltammograms does not exhibit the expected plateau. Indeed, the current reached a maximum value and decreases at higher overpotentials, contrary to what is observed on poly-CoTAPc films.<sup>14</sup> This could be partially explained by the formation of

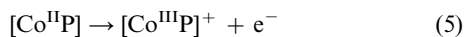


**Fig. 9** Evolution of the hydrodynamic voltammograms of the electro-oxidation of 2-mercaptoethanol ( $1 \text{ mmol L}^{-1}$  in  $0.5 \text{ mol L}^{-1}$  NaOH) with the thickness of electropolymerized poly-CoTAPP (a) and poly-CoTHPP (b) films. Rotation rate  $1600 \text{ rpm}$ , scan rate  $0.05 \text{ V s}^{-1}$ .

adsorbed products that passivate the active sites of the polymer films. One can also notice that at very low potentials (*i.e.* at the foot of the wave), the poly-CoTAPP films are more active than the adsorbed monolayer (in terms of pre-wave current intensity), while at higher potentials the hydrodynamic voltammograms cross each other and the inverse tendency is observed (the adsorbed monolayer is the most active in terms of current intensity). Fig. 10 shows the Tafel plots obtained for the oxidation of 2-ME on poly-CoTAPP and poly-CoTHPP modified vitreous carbon electrodes using current intensity experimentally measured at the very beginning of the catalytic wave (where only kinetic currents exist). The correlation is not linear and the slope changes gradually from values close to 60 mV decade<sup>-1</sup> at low potentials (at the foot of the wave) to 130 mV decade<sup>-1</sup> at higher potentials. This could be attributed to the fact that 2-ME oxidation starts at potentials lower but not far from the potential of the Co<sup>II</sup>/Co<sup>III</sup> redox process of the poly-CoTAPP and poly-CoTHPP films. As the electrocatalytic oxidation of 2-ME progresses within the potential range of the stability of the Co<sup>III</sup> form of the film, one can assume that 2-ME ion can also bind to Co<sup>III</sup>-porphyrins. Thus at low potentials, *i.e.* at the foot of the catalytic wave, the kinetics is controlled by a first fast one-electron transfer involving the cobalt porphyrin (denoted here as [CoP], for simplification) followed by a slow chemical step as indicated below (by assuming that the reaction is a pseudo-first order in 2-ME<sup>4</sup>):



Thus, the oxidation of the adduct in step (2) is probably rapid. This is followed by a slow chemical step (3) involving the rupture of the Co-S bond in the adduct. The thiyl radical then reacts very rapidly in step (4) to give the disulfide. The scheme above explains the Tafel slopes of close to 60 mV decade<sup>-1</sup>. As the potential becomes more positive, the concentration of [Co<sup>II</sup>P] species is rapidly depleted and the surface becomes covered with [Co<sup>III</sup>P]<sup>+</sup> species, which are thermodynamically more stable. The explanation for the slope of 130 mV decade<sup>-1</sup> is that the oxidation of [Co<sup>II</sup>P] to [Co<sup>III</sup>P]<sup>+</sup> becomes rate-controlling since this process is slow. The formation of the supposed [RS-CoP] adduct then occurs between RS<sup>-</sup> and the [Co<sup>III</sup>P]<sup>+</sup> form of the porphyrin which is less active than [Co<sup>II</sup>P], as follows:



The adduct formed in step (6) is then decomposed as in step (3), releasing the thiyl radical. This can also explain the fact that the hydrodynamic voltammograms do not exhibit the expected plateau shape. Thus, the electron transfer mechanisms compete in the examined potential range, with one predominating over the other depending on the potential. This explains the lack of linearity of the Tafel plots.

Note that an alternative mechanism have been previously proposed for the oxidation of 2-ME and other thiols on monolayers of adsorbed cobalt phthalocyanines which involves the Co<sup>II</sup>/Co<sup>I</sup> redox process.<sup>6,40</sup> Fig. 11 (curves a and c) show the evolution of the Soret band of the UV-visible spectra of poly-CoTAPP film (on ITO electrode) upon addition of 2-ME to the aqueous 0.5 mol L<sup>-1</sup> NaOH solution. It appears that 2-ME causes a blue shift of the Soret band, by nearly 10 nm (from 430 to 420 nm, upon addition of 2-ME). Fig. 11 (curve b) shows

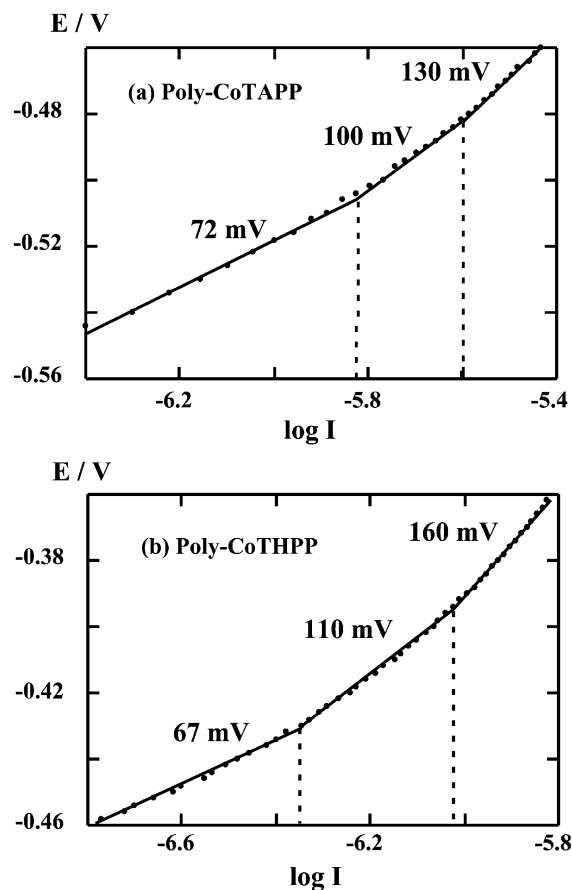


**Fig. 10** Tafel plot for the electro-oxidation of 2-mercaptoethanol (1 mmol L<sup>-1</sup> in 0.5 mol L<sup>-1</sup> NaOH) on (a) poly-CoTAPP modified electrode and on (b) poly-CoTHPP modified electrode (prepared by 24 electropolymerizing scans each).

also that similar blue shift of the Soret band happens upon the electrochemical reduction of the poly-Co<sup>II</sup>TAPP film at -0.65 V. Further reduction of the film at -0.95 V gives a similar UV-visible spectrum. It should be noted that reduction of the film at potential values lower than -1.0 V provokes irreversible alteration of the ITO conducting coating in NaOH solution leading to the depletion of the film. The change in the Soret band from the native form of the film to that of the reduced one obtained at -0.65 V or -0.95 V is reversible. Indeed, the original spectrum can be restored by applying

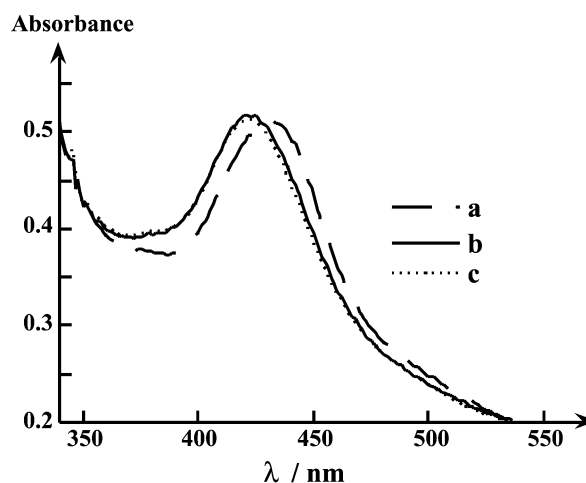


**Fig. 11** Absorption spectra of (a) a native [poly-CoTAPP]<sub>80</sub> film deposited on an ITO electrode immersed in NaOH 0.5 mol L<sup>-1</sup>, (b) [poly-CoTAPP]<sub>80</sub> film after reduction at -0.65 V in 0.5 mol L<sup>-1</sup> NaOH and (c) a native [poly-CoTAPP]<sub>80</sub> film in 0.5 mol L<sup>-1</sup> NaOH + 1 mmol L<sup>-1</sup> 2-mercaptoethanol.

0.1 V. Although the electrochemical reduction of the poly-Co<sup>II</sup>TAPP film at -0.65 V cannot totally lead to the transformation of the porphyrinic film to the Co<sup>I</sup> form, this remarkable result brings a direct indication on a probable intervention of a reduced form of the complex-based film. Such a process may involve the Co<sup>II</sup>/Co<sup>I</sup> redox process, as previously suggested by spectroelectrochemical experiments for adsorbed metallophthalocyanines in presence of cysteine.<sup>40</sup>

## Conclusion

We report here on the first comparative study of the electrochemical formation of cobalt phthalocyanine and porphyrin-based films and their characterization by cyclic voltammetry and electrochemical quartz microbalance measurements. The obtained results clearly show that the accessibility to the redox centers within the electropolymerized films is limited to some extent, probably to the external layers. In particular, this report focuses on the effect of polymer film thickness on the thiol electro-oxidation reaction. Our results show that the porphyrin-based electrodes are active for the electro-oxidation of 2-ME and for the reduction of the corresponding disulfide, as are the phthalocyanine electrodes. However, the electrocatalytic activity of the porphyrin-modified electrodes depends on the films thickness, in contrast to the phthalocyanine-based electrodes: the higher is the thickness the lower is the activation of the thiol in terms of current and of oxidation potential. This can be explained by a lower electronic conductivity of electropolymerized porphyrin-films relative to phthalocyanine-based ones, and the probable participation of the less reactive Co<sup>III</sup> form of the deposited complexes.

## Acknowledgements

The authors are grateful to ECOS-Sud (France) Conicyt (Chile) program C99E03 for financial support for travel expenses. J. H. Z is grateful to Fondecyt (grant 1000218) and Dicyt/Usach (Chile).

## References

- 1 I. Tabushi, *Coord. Chem. Rev.*, 1988, **86**, 1.
- 2 B. Meunier, A. Robert, G. Pratviel and J. Bernadou, in *The Porphyrin Handbook*, ed. K. M. Kadish, K. M. Smith and R. Guilard, Academic Press, San Diego, 2000, vol. 4, ch. 31, pp. 119.
- 3 C. C. Leznoff and A. B. Lever, *Phthalocyanines: Properties and Applications*, Verlag VCH, New York, 1989.
- 4 J. H. Zagal, *Coord. Chem. Rev.*, 1992, **119**, 89.
- 5 J. H. Zagal, M. Gulppi, M. Isaacs, G. Cardenas-Jirón and M. J. Aguirre, *Electrochim. Acta*, 1998, **44**, 1349.
- 6 J. H. Zagal, M. A. Gulppi, C. A. Caro and G. I. Cárdenas-Jirón, *Electrochem. Comm.*, 1999, **1**, 389.
- 7 J. H. Zagal, M. Gulppi, C. Depretz and D. Lelièvre, *J. Porphyrins Phthalocyanines*, 1999, **3**, 35.

- 8 T. R. Ralph, M. L. Hitchman, J. P. Millington and F. C. Walsh, *J. Electroanal. Chem.*, 1994, **375**, 1.
- 9 J. H. Zagal, M. E. Vaschetto and B. A. Retamal, *Int. J. Polym. Mater.*, 1999, **44**, 225.
- 10 X. Qi, P. Baldwin, H. Li and T. F. Guarr, *Electroanalysis (NY)*, 1991, **3**, 119.
- 11 X. Qi and R. P. Baldwin, *Electroanalysis (NY)*, 1994, **6**, 353.
- 12 X. Qi and R. P. Baldwin, *J. Electrochem. Soc.*, 1996, **143**, 1283 and references therein.
- 13 M. Gulppi, F. Bedioui and J. H. Zagal, *Electroanalysis (NY)*, 2001, **13**, 1136.
- 14 S. Griveau, J. Pavez, J. H. Zagal and F. Bedioui, *J. Electroanal. Chem.*, 2001, **497**, 75.
- 15 S. Griveau and F. Bedioui, *Electroanalysis (NY)*, 2001, **13**, 253.
- 16 M. Gulppi, S. Griveau, F. Bedioui and J. H. Zagal, *Electrochim. Acta*, 2001, **43**, 3397.
- 17 M. Pontié, C. Gobin, T. Pauporté, F. Bedioui and J. Devynck, *Anal. Chim. Acta*, 2000, **411**, 175.
- 18 G. Sauerbrey, *Z. Phys.*, 1959, **155**, 206.
- 19 C. Gabrielli, M. Keddam, N. Nadi and H. Perrot, *Electrochim. Acta*, 1999, **44**, 2095.
- 20 M. R. Deakin and D. A. Buttry, *Anal. Chem.*, 1989, **61**, 1147.
- 21 H. P. Dai, Q. H. Wu, S. G. Sun and K. K. Shiu, *J. Electroanal. Chem.*, 1998, **456**, 47.
- 22 B. Bettelheim, B. A. White, S. A. Raybuck and R. W. Murray, *Inorg. Chem.*, 1987, **26**, 1009.
- 23 T. J. Savenije, R. B. M. Koehorst and T. J. Schaafsma, *J. Phys. Chem. B*, 1997, **101**, 720.
- 24 O. El Mouahid, A. Rakotondrainibe, P. Crouigneau, J. M. Léger and C. Lamy, *J. Electroanal. Chem.*, 1998, **455**, 209.
- 25 E. M. Bruti, M. Giannetto, G. Mori and R. Seeber, *Electroanalysis (NY)*, 1999, **11**, 565.
- 26 J. Hayon, A. Taveh and A. Bettelheim, *J. Electroanal. Chem.*, 1993, **359**, 209.
- 27 M. K. Engel, *Rep. Kawamura Inst. Chem. Res.*, 1996/1997, 11–54 and references therein.
- 28 F. Bedioui, M. Voisin, J. Devynck and C. Bied-Charreton, *J. Electroanal. Chem.*, 1991, **297**, 257 and references therein.
- 29 F. Bedioui, J. Devynck and C. Bied-Charreton, *Acc. Chem. Res.*, 1995, **28**, 30 and references therein.
- 30 S. Trévin, F. Bedioui, M. G. Gomez Villegas and C. Bied-Charreton, *J. Mater. Chem.*, 1997, **7**, 923.
- 31 J. Basu and K. K. Rohatgi-Mukherjee, *Sol. Energy Mater.*, 1991, **21**, 317.
- 32 Y. Tse, P. Janda, H. Lam, J. Zhang, W. Pietro and A. B. P. Lever, *J. Porphyrins Phthalocyanines*, 1997, **1**, 3 and references therein.
- 33 B. A. White and R. W. Murray, *J. Am. Chem. Soc.*, 1987, **109**, 2576.
- 34 N. A. Surridge, J. C. Jernigan, E. F. Dalton, R. P. Buck, M. Watanabe, H. Zhang, M. Pinkerton, T. T. Wooster, M. L. Longmire, J. S. Facci and R. W. Murray, *Faraday Discuss. Chem. Soc.*, 1989, **88**, 1.
- 35 R. W. Murray, *Electroanal. Chem.*, 1984, **13**, 191.
- 36 F. Daire, F. Bedioui and J. Devynck, *J. Electroanal. Chem.*, 1987, **224**, 95.
- 37 A. Bard and L. Faulkner, in *Electrochemical Methods: Fundamentals and Applications*, Wiley & Sons, New York, 2nd edn., 2001.
- 38 H. H. Girault, in *Electrochimie Physique et Analytique*, Presses Polytechniques et Universitaires Romandes, Lausanne, 2001.
- 39 J. H. Zagal, M. Gulppi and G. Cardenas-Jirón, *Polyhedron*, 2000, **19**, 2255.
- 40 R. O. Lezna, S. Juanto and J. H. Zagal, *J. Electroanal. Chem.*, 1998, **452**, 221.